Collective motion of oscillatory walkers

Takahiro Ezaki,[1,2,*] Ryosuke Nishi,[3,4] Daichi Yanagisawa,[5] and Katsuhiro Nishinari[6]

[1]*Department of Aeronautics and Astronautics, School of Engineering, The University of Tokyo,*
7-3-1 Hongo, Bunkyo-ku, Tokyo 113-8656, Japan

[2]*Japan Society for the Promotion of Science, 5-3-1 Ichibancho, Kojimachi, Chiyoda-ku, Tokyo 102-0083, Japan*

[3]*National Institute of Informatics, 2-1-2 Hitotsubashi, Chiyoda-ku, Tokyo 101-8430, Japan*

[4]*JST, ERATO, Kawarabayashi Large Graph Project, 2-1-2 Hitotsubashi, Chiyoda-ku, Tokyo 101-8430, Japan*

[5]*College of Science, Ibaraki University, 2-1-1 Bunkyo, Mito, Ibaraki 310-8512, Japan*

[6]*Research Center for Advanced Science and Technology, The University of Tokyo,*
4-6-1 Komaba, Meguro-ku, Tokyo 153-8904, Japan

We study a system of interacting self-propelled particles whose walking velocity depends on the stage of the locomotion cycle. The model introduces a phase equation in the optimal velocity model for vehicular traffic. We find that the system exhibits novel types of flow: synchronized free flow, phase-anchoring free flow, orderly jam flow, and disordered jam flow. The first two flows are characterized by synchronization of the phase, while the others do not have the global synchronization. Among these, the disordered jam flow is very complex, although the underlying model is simple. This phenomenon implies that the crowd behavior of moving particles can be destabilized by coupling their velocity to the phase of their motion. We also focus on "phase-anchoring" phenomena. They strongly affect particle flow in the system, especially when the density of particles is high.

I. INTRODUCTION

The movements of all animate things, such as the walking of humans, flapping of birds, and swimming of fish, are restricted by their locomotion [1]. Since the collective motion of self-propelled particles (SPP) began to attract interest [2–4], many studies have been conducted in various contexts [5], including pedestrian crowds [6–14], bird flocks [15], and insect swarms [16,17]. However, the effect of locomotion on macroscopic behavior remains an open question. In fact, recent experiments in the field of pedestrian dynamics suggest that the oscillatory motion of pedestrian walking may have a significant effect on overall dynamics [13,14]. Jelić *et al.* studied the collective dynamics of pedestrians walking in a line, focusing on bilateral oscillations during walking [13]. From fluctuating trajectories, they obtained the phase of locomotion and investigated the interaction between neighboring pedestrians. Furthermore, Yanagisawa *et al.* [14] reported that the synchronization of locomotion phase among pedestrians may increase the total flux. Here the "phase" is a mapping from each stage of locomotion to a real number $\phi \in \mathbb{R}/2\pi\mathbb{Z}$. Unlike the situation in the vehicular traffic, this phase is strongly related to the velocity of walkers.

In this paper, we propose a simple model that describes particle-following behavior, phase-velocity coupling, and phase-phase coupling. Particle-following behavior is implemented by the optimal velocity (OV) model [18] for vehicular traffic. This model is known to demonstrate the phase transition from free flow to jam flow, which is highly tractable in mathematical analyses. Phase-phase coupling is considered within the framework of the Kuramoto model [19], a paradigmatic model describing synchronization phenomena in nature. In the present study we assume that the phases of successive particles

tend to synchronize, which is experimentally suggested when pedestrians walk in a dense crowd [13]. Since each walker follows its predecessor and ignores its successors, the interaction is unidirectional and local. In contrast, other studies have been mainly devoted to globally coupled oscillators or locally but bidirectionally coupled oscillators [20,21]. Note that we do not consider detailed modeling of actual animals; instead, we concentrate on ideal particles called oscillatory walkers (OWs). Although here we assume the interaction between particles is through their headway distances, it could depend also on their (relative) velocities, which is beyond the scope of this paper.

In spite of its simplicity, the OW model presents a rich behavior, including a novel type of jam [Fig. 1(b)]. We report its fundamental characteristic and give insight into its collective locomotion.

The rest of the paper is organized as follows. The next section is devoted to define the model. In Sec. III we summarize the dynamics of the model. To understand its destabilization phenomena, theoretical analyses are performed in Sec. IV. Finally we summarize these results in the final section.

II. MODEL

Consider N particles, labeled $n = 1, \ldots, N$ from the left walking to the right on a one-dimensional ring. We impose periodic boundary conditions [particle $(N + 1)$ particle is identical to particle 1]. The velocity of the nth walker ($\dot{x}_n$) is determined by the following equation:

$$\ddot{x}_n = a\{V(\Delta x_n) + A(\cos\phi_n + 1) - \dot{x}_n\}, \tag{1}$$

where $V(\Delta x_n)$ is the optimal velocity determined for headway distance ($\Delta x_n = x_{n+1} - x_n$) [18]. Each walker adapts its velocity to this optimal velocity with an adaptation intensity (the reciprocal of the reaction time) a. The effect of locomotion is represented by the oscillation term $A(\cos\phi_n + 1)$. The quantity A is the magnitude of the fluctuations in the target
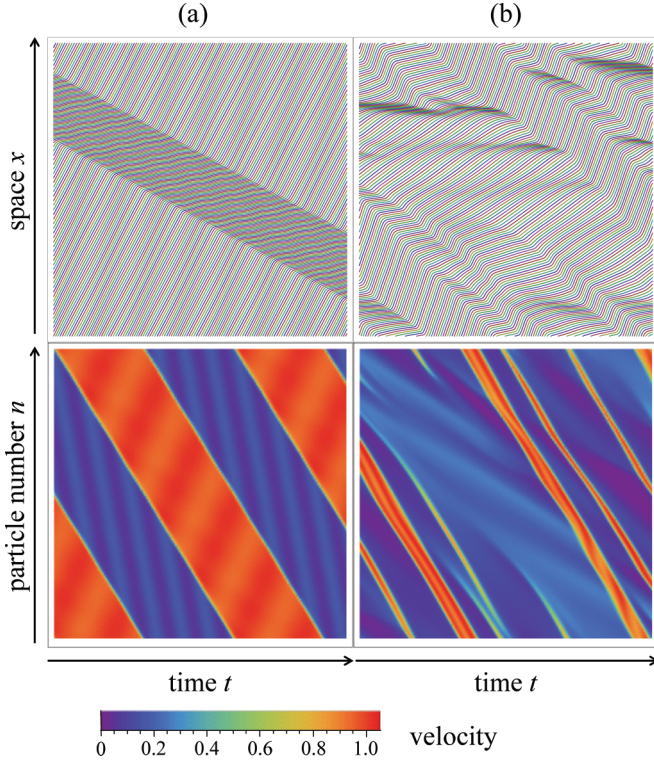
*ezaki@jamology.rcast.u-tokyo.ac.jp

FIG. 1. (Color online) Space-time diagrams (top) and velocity-time diagrams (bottom) for orderly jam flow (left, $\rho = 2.0, K = 5.0$, $A = 0.05$) and disordered jam flow (right, $\rho = 3.0, K = 1.0$, $A = 0.05$). Bold lines indicate the trajectory of the 50th walker. The small regular waves in orderly jam flow correspond to phase anchoring.

velocity, which is set to a small value. The fluctuation phase ϕ_n is determined by

$$\dot{\phi}_n = \omega(\Delta x_n) + K \sin \Delta \phi_n. \tag{2}$$

Here we assume that the ideal angular velocity $\omega(\Delta x_n)$ is defined by a function similar to the ideal walking velocity $V(\Delta x_n)$, i.e., using a normalized optimal velocity (NOV) function $U(\Delta x_n)$, we can express $\omega(\Delta x_n) = \Omega_M U(\Delta x_n)$ and $V(\Delta x_n) = V_M U(\Delta x_n)$. We further impose the condition that when the headway distance is large enough, particles walk with a steady angular velocity Ω_M and velocity V_M, and for small Δx_n, $U(\Delta x_n) \sim 0$ to stop. To capture these assumptions, the NOV function is set to be a differentiable and monotonically increasing function that is asymptotic to 0 as $\Delta x_n \to 0$ and to a positive constant as $\Delta x_n \to \infty$. We use the following form of the NOV function when actual calculations are needed: $U(\Delta x_n) = c_1[\tanh(c_2 \Delta x_n - c_3) + \tanh c_3]$ with the positive parameters c_1, c_2, and c_3. $U(\Delta x_n)$ is a monotonic increasing function such that $U(0) = 0$ and $U(\infty) = c_1[1 + \tanh c_3]$. The quantity c_3/c_2 corresponds to its inflection point, and c_1 and c_3 determines its height given by $c_1[1 + \tanh c_3]$. Here we set $c_1 = 0.5$, $c_2 = 5$, and $c_3 = 2.5$.

The second term on the right hand side (rhs) of Eq. (2) represents the synchronous interaction of successive walkers, whose intensity is $K > 0$. When the phase difference $\Delta \phi_n = \phi_{n+1} - \phi_n$ is zero and the walkers are uniformly distributed, they walk with a steady velocity and rhythm (synchronized free flow). In this paper, we restrict the model parameters to $a = 3$, $V_M = 1$, $\Omega_M = 1$, and $N = 100$. We vary the particle density $\rho = N/L$ by changing the system length L.

III. DYNAMICS OF THE OW MODEL

The OW model has four types of flow: synchronized free flow (SFF), phase-anchoring free flow (PFF), orderly jam flow (OJF), and disordered jam flow (DJF). "Phase anchoring" occurs when phase differences $\Delta \phi_n$ are fixed at a common value $\Delta \phi_0 \in (-\pi, \pi]$. When the effects of distance between the walkers are negligible, the model reduces to the Kuramoto model with local interactions. Then the states $\Delta \phi_n = $ const.,
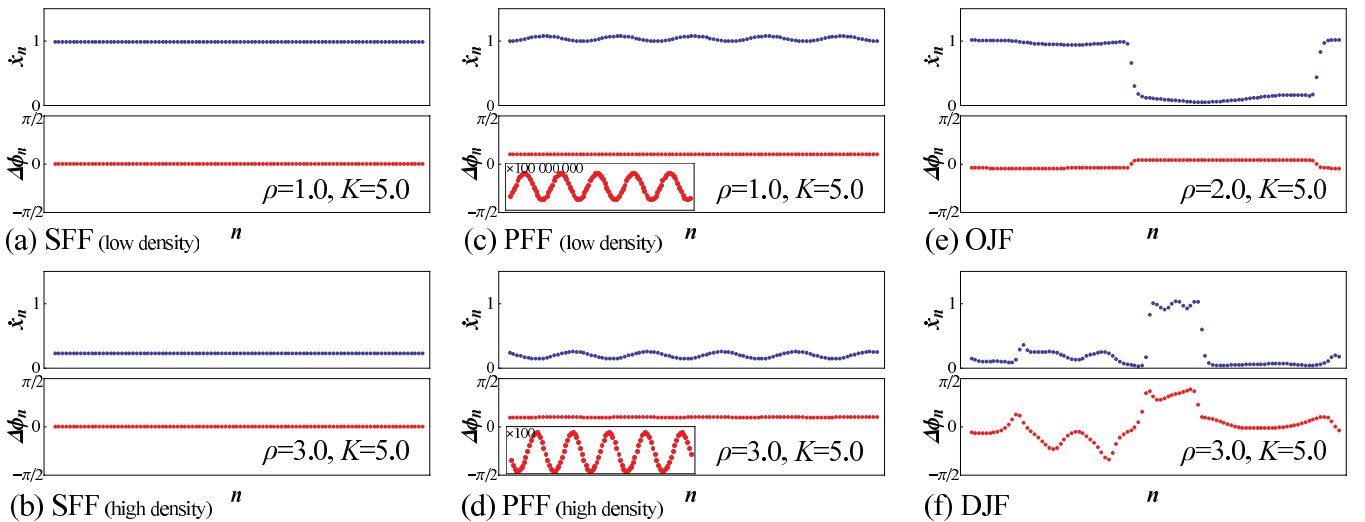

FIG. 2. (Color online) Snapshots of velocity and phase difference for $A = 0.05$. On the abscissae, n represents the particle number. Panels (a) and (b) are for synchronized free flow (SFF), panels (c) and (d) are for phase-anchoring free flow (PFF), panel (e) is for orderly jam flow (OJF), and panel (f) is for disordered jam flow (DJF). Wavy shapes of velocity in (c), (d), and (e) stem from the constant phase difference. In PFF (c) and (d), the phase differences are almost constant, but slight fluctuations occur, as shown in the insets. For $a = 3.0$ we set, $\rho = 1.0, 2.0$, and 3.0 correspond to low-, middle-, and high-density regimes, respectively. As explained in the text, the middle-density regime has OJF only.

in which all angular velocities are identical, are stable over a certain range of $\Delta\phi_0$. This property is inherited by the OW model; however, as can be easily verified, the states $\Delta\phi_n = \text{const.} \neq 0$ cannot be realized exactly because of the effects of spatial structure. Actually, each phase difference fluctuates slightly around $\Delta\phi_0$ as depicted in Figs. 2(c) and 2(d).

Before going into detail, we briefly summarize the dynamics in the system. First, similar to vehicular traffic flow, the model has phase transitions between free flow and (orderly) jam flow; these are caused by increases in the density of walkers. When the density is small ($\rho < \rho_{cr,1}$) free flow is stable and a jam cannot develop. At middle densities $\rho_{cr,1} < \rho < \rho_{cr,2}$ free flow is no longer stable and small perturbations grow into a jam; this is called OJF [Figs. 1(a) and 2(e)]. At high densities $\rho_{cr,2} < \rho$, the system regains stability for free flow. In the free flow regime, the OW model has two types of flow: SFF [Figs. 2(a) and 2(b)] and PFF [Figs. 2(c) and 2(d)]. These flows are locally stable, and all transient flows are asymptotic to either SFF or PFF in the low-density regime, depending on the initial condition. In contrast, in the high-density regime SFF is always locally stable, while PFF can be destabilized for some parameter regimes, resulting in another type of jam.

In the OJF of the middle-density regime, the separation of phase differences occurs. As shown in Fig. 2(e), the phase differences become almost constant in each region. This phase anchoring is produced by the spatial structure of OJF, and it also depends on K and the initial conditions.

In addition to these states, another nontrivial phenomenon emerges in the high-density regime, namely disordered jam flow (DJF). This is complex jam flow induced by strong coupling between ϕ_n and x_n. As shown in Figs. 1(b) and 2(f), no steady pattern occurs, and small jams propagate with different velocities and even disappear and reappear. The four types of flow correlate with density as in Table I.

Now we investigate the system in detail.

A. Phase-anchoring phenomena

We first focus on phase-anchoring phenomena. In this paper, we use the following definition for PFF: (i) Each $\Delta\phi_n$ and Δx_n periodically fluctuates around a certain phase difference $\Delta\phi_0$ (const.) and headway distance $\Delta x_0 = \frac{1}{\rho}$, respectively. (ii) The ranges of these fluctuations are small ($\ll |\Delta\phi_0|$).

The effects of phase anchoring are significant, especially when the density of walkers is high. In this regime, since each Δx_n and $\omega(\Delta x_n)$ is small, the dependence of the system dynamics on phase becomes relatively large. One intriguing
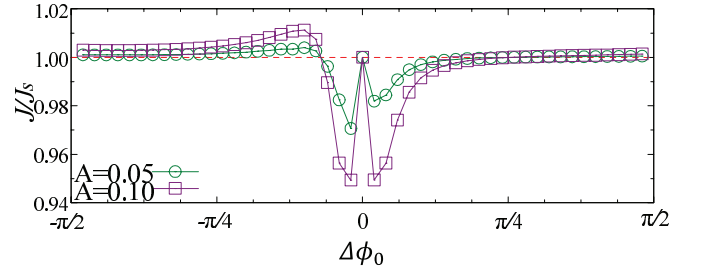

FIG. 3. (Color online) Relationship between flux and phase difference for the case of $\rho = 4.0$ and $K = 5.0$ (PFF in the high-density regime). Here the flux is normalized by the SFF value ($\Delta\phi_0 = 0$).

feature is the relationship between phase anchoring and the flux of walkers. We show the relation between flux and phase difference $\Delta\phi_0$ in Fig. 3. Flux is defined as the product of density and average velocity, averaged over time $J = \langle \rho\bar{x} \rangle$. For SFF, we can calculate the flux as $J_s = \rho[V(\frac{1}{\rho}) + A]$. Simulation results indicate that for small phase delays and advances the flux is decreased, but for large phase differences the flux increases, especially when the phase advances ($\Delta\phi_0 < 0$). In addition, as expected, the effect of the phase difference is conspicuous when the intensity of the coupling parameter A is large. Although phase-anchoring can be observed in the low-density regime, there is little change in the flux because when the headway distance is large, fluctuations in the phase anchoring do not influence the angular velocity through the term $\omega(\Delta x_n) \simeq \Omega_M$. In PFF, each Δx_n oscillates with a certain phase that differs from the walking phase ϕ_n. This difference distorts the trajectory of walkers from that in SFF (represented by a sine curve), leading to decreases and increases in the flux. (See also Appendix B.)

B. Disordered jam flow

For small K and high density ρ, free flow allows only synchrony ($\Delta\phi_0 = 0$) and PFF becomes unstable, and a highly complex flow appears. This flow is phenomenologically distinct from OJF, which is already observed in the OV model. Instead, it originates from the strong coupling between x_n and ϕ_n. In DJF, small jams locally appear and disappear intermittently, and no stationary state is reached [Fig. 1(b)]. Further, we can no longer observe regular patterns in x_n, $\dot{x}_n$, or $\Delta\phi_n$ [Figs. 1(b) and 2(f)]. Figure 4 shows a complex limit cycle of DJF in the $(\Delta x_1, \dot{x}_1)$ plane; the figure also shows the trajectory of the jam flow in the OV model. In the quasiperiodic trajectory of DJF, we can see distinctive patterns, especially at its edges.

IV. THEORETICAL ANALYSES

Next we discuss the stability conditions for each flow. To understand the destabilization of steady free flow, $(x_n^{(0)}, \phi_n^{(0)})$, we investigate how the flow responds to small perturbations. For a small perturbation $x_n = x_n^{(0)} + \epsilon_n, \phi_n = \phi_n^{(0)} + \delta_n$, the system equations (1) and (2) linearize to

$$\dot{\epsilon}_n/a = -\epsilon_n + V_M U'\left(\Delta x_n^{(0)}\right)\Delta\epsilon_n - A\sin\phi_n^{(0)}\delta_n, \quad (3)$$

$$\dot{\delta}_n = K\cos\Delta\phi_n^{(0)}\Delta\delta_n + \Omega_M U'\left(\Delta x_n^{(0)}\right)\Delta\epsilon_n, \quad (4)$$

TABLE I. Classification of flows. Each tick indicates the existence of the flow in the density regime.

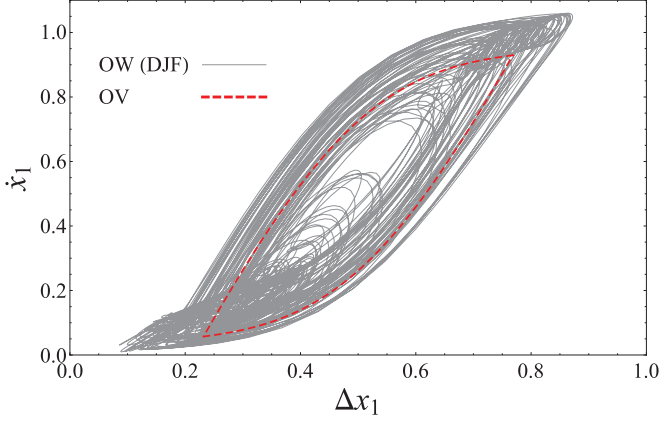|		Density		
		Low	Middle	High
Free flow	Synchronized free flow (SFF)	✓		✓
	Phase-anchoring free flow (PFF)	✓		✓
Jam flow	Orderly jam flow (OJF)		✓	
	Disordered jam flow (DJF)			✓

FIG. 4. (Color online) Headway-velocity trajectory for DJF ($A = 0.05$, $\rho = 3.0$, and $K = 1.0$). The red broken line represents the trajectory of jam flow in the OV model ($A = 0$, $\rho = 2.0$).

with $U'(\Delta x_n^{(0)}) = \frac{\partial U}{\partial \Delta x}|_{\Delta x = \Delta x_n^{(0)}}$. When all walkers are uniformly synchronized, namely, $\Delta x_n^{(0)} = L/N = 1/\rho$, $\phi_n^{(0)} = \Omega_M U(1/\rho)t \equiv \dot{\phi}_s t$, Eqs. (3) and (4) simplify to

$$\ddot{\epsilon}_n/a = -\epsilon_n + V_M U'(1/\rho)\Delta\epsilon_n - A\sin(\dot{\phi}_s t)\delta_n, \quad (5)$$

$$\dot{\delta}_n = K\Delta\delta_n + \Omega_M U'(1/\rho)\Delta\epsilon_n. \quad (6)$$

Here we assume that $\dot{\phi}_s t$ is a fast variable compared to the growth rate of the perturbation, i.e., ϵ, δ, and their derivatives are constant for each period $T = \frac{2\pi}{\dot{\phi}_s}$. By integrating Eq. (5) over this period, we can eliminate the vibrational term, leaving

$$\ddot{\epsilon}_n/a = -\epsilon_n + V_M U'(1/\rho)\Delta\epsilon_n, \quad (7)$$

which is the linearized OV model. Now the stability condition is given by $V_M U'(1/\rho) < \frac{a}{2}$ [22]. When ϵ_n does not grow in Eq. (7), Eq. (6) gives the condition on K as $K > 0$.

For PFF, the analysis is not straightforward; we start with Eq. (4). By ignoring the coupling between ϵ_n and δ_n as well as the fluctuations in the phase difference [i.e., $\Delta\phi_n^{(0)} \simeq \Delta\phi_0$], we obtain

$$\dot{\delta}_n = K\cos(\Delta\phi_0)\Delta\delta_n. \quad (8)$$

From this equation, we can find the stability condition $|\Delta\phi_0| < \frac{\pi}{2}$. Additionally, since the system is periodic ($\phi_{N+1} = \phi_1$), the condition $N\Delta\phi_0 = 2m\pi$ ($m = \pm 1, \pm 2, \dots$) must be satisfied. To summarize, stable $\Delta\phi_0$ can take the discrete values of $\Delta\phi_0 = 0, \pm\frac{2\pi}{N}, \pm\frac{4\pi}{N}, \dots, \pm(\frac{\lfloor N/2\rfloor - 2}{N})\pi$, where $\lfloor Y \rfloor$ is the floor function giving the maximum integer not larger than Y. These conditions were verified by numerical simulations. On the other hand, the coupling behavior of ϵ_n and δ_n is determined by the final term in Eq. (3). If the time integral $\int_0^{T'}\sin\phi_n^{(0)}dt \neq 0$ (i.e., if the sine function is "distorted"), the system can destabilize. This distortion is also observed as a change of flux in the high-density regime (Fig. 3, see also the approximate analyses in Appendix B). From these facts, we conclude that the high-density regime leads to coupling in the stability equation, which may result in DJF.

In Fig. 5 we illustrate the phase diagrams of the system by simulations, using the expression for PFF ($x_{n,1}, \phi_{n,1}$) (whose derivation is found in Appendix A) as initial conditions to see
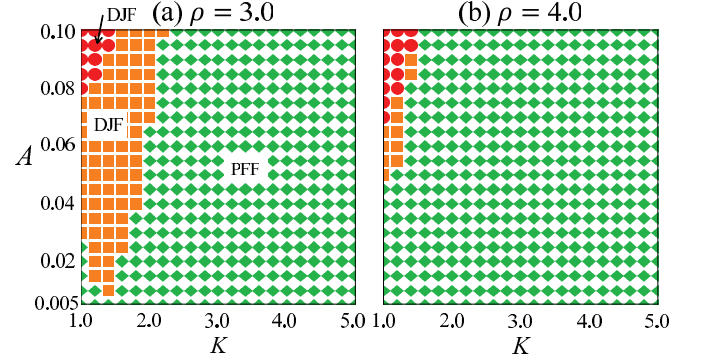

FIG. 5. (Color online) Phase diagram in the high-density regime. Initial conditions are given by the expression of PFF with $\Delta\phi_0 = \frac{2\pi}{100}$, $(x_{n,1}, \phi_{n,1})$. If we take SFF as initial conditions ($\Delta\phi_0 = 0$), the flow is always stable. Green diamonds indicate the parameter region where PFF is stable. Orange squares and red circles correspond to the emergence of DJF, and the latter include collisions of walkers. The same diagrams for low- and middle-density regimes only show PFF and OJF, respectively.

whether the flow is stable or not

$$\begin{aligned}
x_{n,1} &= v_0 t + \frac{n}{\rho} + \frac{Aa}{\dot{\phi}_0\sqrt{a^2 + \dot{\phi}_0^2}}\sin\Psi(t) \\
&\quad + \frac{2Aa^2 V'(\frac{1}{\rho})\sin(\frac{\Delta\phi_0}{2})}{\dot{\phi}_0^2(a^2 + \dot{\phi}_0^2)}\sin\left(\Psi(t) - \varphi_0 + \frac{\Delta\phi_0}{2}\right),
\end{aligned}$$

$$\begin{aligned}
\phi_{n,1} &= \dot{\phi}_0 t + \Delta\phi_0 n \\
&\quad + \frac{2Aa\omega'(\frac{1}{\rho})\sin\frac{\Delta\phi_0}{2}}{\dot{\phi}_0^2\sqrt{a^2 + \dot{\phi}_0^2}}\sin\left(\Psi(t) + \frac{\Delta\phi_0}{2}\right),
\end{aligned}$$

where $v_0 = V(1/\rho) + A$, $\dot{\phi}_0 = \omega(1/\rho) + K\sin\Delta\phi_0$, $\varphi_0 = \tan^{-1}(\dot{\phi}_0/a)$, and $\Psi(t) = \dot{\phi}_0 t - \varphi_0 + \Delta\phi_0 n$. It is found that the system destabilizes for small K and large A, and for especially large values of A, particles even collide with each other in DJF. Thus we can conclude that the increase of A and K are connected to the destabilization and stabilization of the system, respectively. In addition, the increase of particle density reduces the DJF regime because it decreases the space for the "over acceleration" of particles that is indispensable for DJF.

V. CONCLUSIVE DISCUSSION

In summary, we have proposed a simple model to show that the restriction coming from locomotion largely affects the collective behavior of SPPs. The model has various types of flow, including a novel type of complex flow called disordered jam flow (DJF). Disordered jam flow appears when the particle density is high; this flow is caused by coupling between the velocities and phases of particles. We also find that the particle flux is strongly affected by phase anchoring. On the other hand, some issues remain to be clarified in future studies. These include synchronization phenomena on inhomogeneous distributions of intrinsic optimal velocity and angular velocity, quantitative analysis for phase anchoring and its effect on flux,

and so on. These points should be addressed in detail in future works.

Although pedestrian locomotion in a crowd is not yet fully understood, a real pedestrian may adapt the crowd velocity and step length by considering the environment of other pedestrians (not only the nearest predecessor). Furthermore, the environment may affect a pedestrian through a strong psychological repulsive force [11]. We believe that by including the effects of phase, models for pedestrians and other animals can be improved. Moreover, the synchronization of pedestrians through a bridge [23,24] might be an interesting problem. It is also attractive to extend this model to two dimensions using the two-dimensional OV model [25], the generalization of which would require additional rules of phase synchronization.

APPENDIX A: APPROXIMATE DESCRIPTION OF PFF

In this section we give equations of a particle trajectory in PFF approximately. The trajectory satisfies the following system equations:

$$\ddot{x}_n = a\{V(\Delta x_n) + A(\cos\phi_n + 1) - \dot{x}_n\}, \tag{A1}$$

$$\dot{\phi}_n = \omega(\Delta x_n) + K\sin\Delta\phi_n. \tag{A2}$$

First, we assume that the deviation of each Δx_n is small compared to its absolute value and that the phase difference $\Delta\phi_n$ is constant ($\Delta\phi_0$). In this assumption, $\Delta x_n = \frac{1}{\rho}, \dot{\phi}_n = \omega(\frac{1}{\rho}) + K\sin\Delta\phi_0 \equiv \dot{\phi}_0$(const.). Then, the system equations (A1) and (A2) can be easily integrated as follows:

$$\phi_{n,0} = \dot{\phi}_0 t + \Delta\phi_0 n, \tag{A3}$$

$$x_{n,0}(t) = \frac{Aa}{\dot{\phi}_0\sqrt{a^2 + \dot{\phi}_0^2}}\sin(\dot{\phi}_0 t - \varphi_0 + \Delta\phi_0 n) + v_0 t + \frac{n}{\rho}, \tag{A4}$$

$$\dot{x}_{n,0}(t) = \frac{Aa}{\sqrt{a^2 + \dot{\phi}_0^2}}\cos(\dot{\phi}_0 t - \varphi_0 + \Delta\phi_0 n) + v_0. \tag{A5}$$

Here we put $v_0 \equiv V(\frac{1}{\rho}) + A$ and $\varphi_0 = \tan^{-1}(\frac{\dot{\phi}_0}{a})$. These equations give exact trajectories of particles when $\Delta\phi_0 = 0$ (SFF).

However, these expressions are not enough for understanding the dynamics of PFF in high-density cases. We next give a more accurate approximation based on these equations; the deviation of particle distance Δx_n is taken into consideration, while the deviation of phase-difference is still ignored. Using the previous result we approximately give $\Delta x_n = x_{n+1,0} - x_{n,0}$ in advance

$$\Delta x_n - \frac{1}{\rho} \simeq \frac{Aa}{\dot{\phi}_0\sqrt{a^2 + \dot{\phi}_0^2}}[\sin(\dot{\phi}_0 t - \varphi_0 + \Delta\phi_0 n + \Delta\phi_0) - \sin(\dot{\phi}_0 t - \varphi_0 + \Delta\phi_0 n)] \tag{A6}$$

$$= \frac{2Aa\sin\frac{\Delta\phi_0}{2}}{\dot{\phi}_0\sqrt{a^2 + \dot{\phi}_0^2}} \times \cos\left(\dot{\phi}_0 t - \varphi_0 + \Delta\phi_0 n + \frac{\Delta\phi_0}{2}\right) \tag{A7}$$

$$= A_\Delta\cos\left(\dot{\phi}_0 t - \varphi_0 + \Delta\phi_0 n + \frac{\Delta\phi_0}{2}\right), \tag{A8}$$

where A_Δ is the amplitude of the oscillation of Δx_n. Then the equation for ϕ_n (A2) is now rewritten as

$$\dot{\phi}_{n,1} = \omega(1/\rho) + K\sin\Delta\phi_0 + \omega'(1/\rho)A_\Delta \times \cos\left(\dot{\phi}_0 t - \varphi_0 + \Delta\phi_0 n + \frac{\Delta\phi_0}{2}\right), \tag{A9}$$

which can be solved as

$$\phi_{n,1} = \phi_{n,0} + \frac{2Aa\omega'(1/\rho)\sin\frac{\Delta\phi_0}{2}}{\dot{\phi}_0^2\sqrt{a^2 + \dot{\phi}_0^2}} \times \sin\left(\dot{\phi}_0 t - \varphi_0 + \Delta\phi_0 n + \frac{\Delta\phi_0}{2}\right). \tag{A10}$$

Here we assumed $\Delta x_n - \frac{1}{\rho} \ll 1$. In the same manner, we can derive a more accurate expression for Δx_n as follows:

$$x_{n,1} = x_{n,0} + \frac{2Aa^2 V'(1/\rho)\sin\left(\frac{\Delta\phi_0}{2}\right)}{\dot{\phi}_0^2\left(a^2 + \dot{\phi}_0^2\right)} \times \sin\left(\dot{\phi}_0 t - 2\varphi_0 + \Delta\phi_0 n + \frac{\Delta\phi_0}{2}\right). \tag{A11}$$

Note that the effect of these correction terms increases as $|\dot{\phi}_0|$ (or $\Delta\phi_0$) becomes small (large), namely, the first approximations presented in this section do not agree with
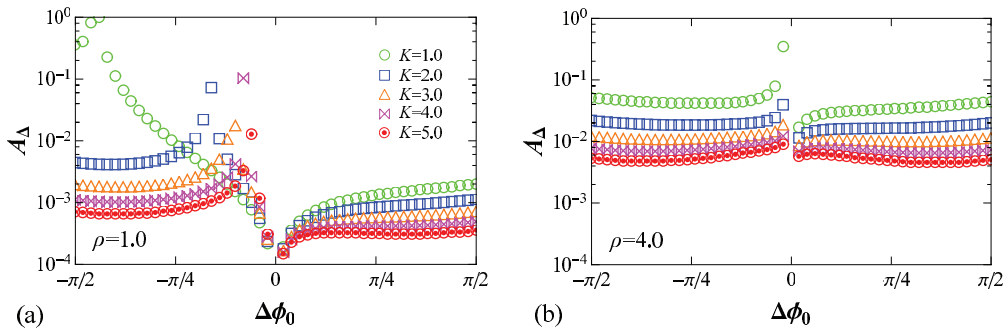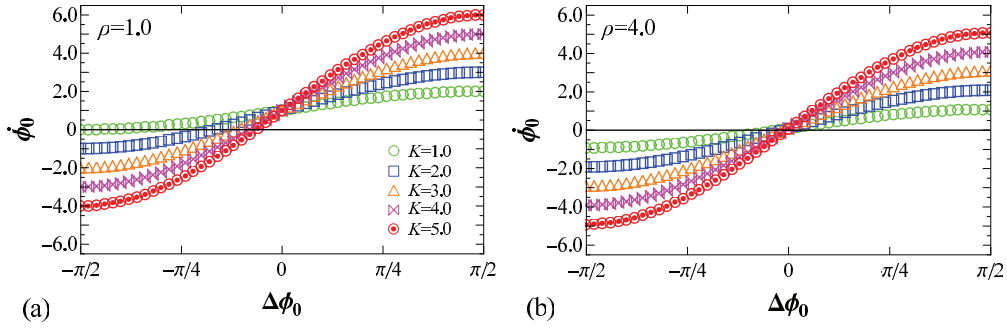

FIG. 6. (Color online) Relationship between A_Δ and $\Delta\phi_0$ for the cases of $A = 0.05$.

FIG. 7. (Color online) Relationship between $\dot{\phi}_0$ and $\Delta\phi_0$ for the cases of $A = 0.05$.

actual trajectories (see also Fig. 7). As shown in Fig. 6, the approximation is valid for large K and small positive $\Delta\phi_0$.

We improved the approximation using $(x_{n,0}, \phi_{n,0})$ to obtain $(x_{n,1}, \phi_{n,1})$. In the same procedure, further improvement can be made by calculating the series of trigonometric functions $(x_{n,k+1}, \phi_{n,k+1})$ from $(x_{n,k}, \phi_{n,k})$ if their amplitude is small enough to allow the Taylor expansion of the optimal-velocity functions, while it is far more difficult to describe the system where this assumption is not valid.

In the main text we used $x_{n,1}$ and $\phi_{n,1}$ as initial conditions to plot the phase diagrams.
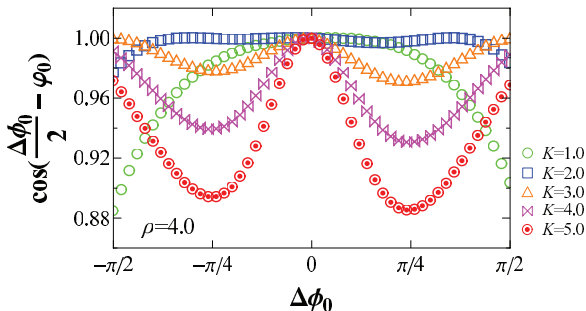
APPENDIX B: DISTORTION OF TRAJECTORY AND ITS EFFECT ON PARTICLE FLUX

Average velocity of a particle in a steady flow is given by integrating Eq. (A1) over a period of one "step," $\mathcal{T}$:

$$\frac{1}{\mathcal{T}} \int_{\mathcal{T}} \dot{x}_n dt = \frac{1}{\mathcal{T}} \int_{\mathcal{T}} V(\Delta x_n) dt + A$$
$$+ \frac{1}{\mathcal{T}} \int_{\mathcal{T}} A \cos\phi_n dt. \quad \text{(B1)}$$

By using the first-order approximation $(x_{n,0}, \phi_{n,0})$ and assuming that the amplitudes of Δx_n and A_Δ are small enough, we can estimate the average velocity as

$$\frac{1}{\mathcal{T}} \int_{\mathcal{T}} \dot{x}_n dt \simeq v_0 + \frac{1}{T} \int_{\mathcal{T}} A \cos\phi_{n,1} dt. \quad \text{(B2)}$$

Therefore the particle flux in PFF is affected by the fluctuation of $\dot{\phi}_n$ from $\phi_{n,0}$, by which the final integral in the above equation remains nonzero. Now the degree of the distortion is characterized by Eq. (A9). For example, we see the difference between the functions $\cos\phi_{n,0}$ and $\cos\phi_{n,1}$ when the focal phase difference $\Delta\phi_0$ is a small positive number that leads to small $\dot{\phi}_0$. The former function is at its maximum at $\dot{\phi}_0 t + \Delta\phi_0 n = 2m\pi$, at which the phase velocity of the modified approximation $\phi_{n,0}$ is faster than $\dot{\phi}$:

$$\dot{\phi}_{n,1}|_{\phi_{n,0}=2m\pi} = \dot{\phi}_0 + \frac{2Aa\omega'(1/\rho)\sin\frac{\Delta\phi_0}{2}}{\dot{\phi}_0\sqrt{a^2 + \dot{\phi}_0^2}}$$
$$\times \cos\left(\frac{\Delta\phi_0}{2} - \varphi_0\right) > \dot{\phi}_0. \quad \text{(B3)}$$

The contribution of the phase difference $\frac{\Delta\phi_0}{2} - \varphi_0$ is depicted in Fig. 8. In the same manner, we can find that when $\phi_0 = (2m+1)\pi$, $\dot{\phi}_{n,1}$ is slower than $\dot{\phi}$. Consequently, the positive part of the cosine function (that corresponds to the approximation $\phi_{n,0}$) shrinks while its negative part is amplified (see Fig. 9), resulting in a smaller value of the integral, and the particle flux decreases as shown in Fig. 3 in the main text. Thus the decrease in the flux around $\Delta\phi_0 = 0$ can be explained in terms of the interaction between oscillations. However, this theory cannot account for the cases of $J/J_s > 1$, for which we have to take the large deformations of trajectories into account.

FIG. 8. (Color online) $\cos\left(\frac{\Delta\phi_0}{2} - \varphi_0\right)$ vs $\Delta\phi_0$ for the cases of $\rho = 4.0$ and $A = 0.05$.
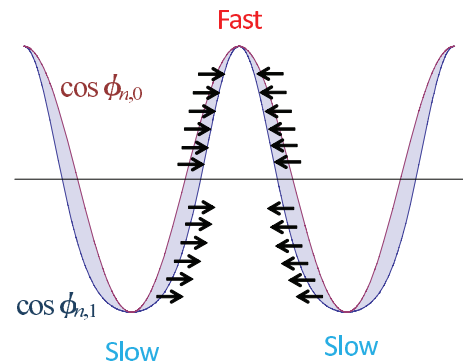
FIG. 9. (Color online) Effect of fluctuation of $\dot{\phi}_n$ on the distortion of the cosine function.

[1] M. R. Alexander, *Locomotion of Animals* (Blackie and Son, Glasgow, Scotland, 1982).

[2] T. Vicsek, A. Czirok, E. Ben-Jacob, I. Cohen, and O. Shochet, Phys. Rev. Lett. **75**, 1226 (1995).

[3] J. Toner and Y. H. Tu, Phys. Rev. Lett. **75**, 4326 (1995).

[4] J. Toner and Y. H. Tu, Phys. Rev. E **58**, 4828 (1998).

[5] T. Vicsek and A. Zafeiris, Phys. Rep. **517**, 71 (2012).

[6] D. Helbing, I. Farkas, and T. Vicsek, Nature (London) **407**, 487 (2000).

[7] D. Helbing, Rev. Mod. Phys. **73**, 1067 (2001).

[8] A. Schadschneider, D. Chowdhury, and K. Nishinari, *Stochastic Transport in Complex Systems: From Molecules to Vehicles* (Elsevier, Amsterdam, 2010).

[9] M. Chraibi, A. Seyfried, and A. Schadschneider, Phys. Rev. E **82**, 046111 (2010).

[10] C. Burstedde, K. Klauck, A. Schadschneider, and J. Zittartsz, Physica A **295**, 507 (2001).

[11] T. Ezaki, D. Yanagisawa, K. Ohtsuka, and K. Nishinari, Physica A **391**, 291 (2012).

[12] T. Ezaki, D. Yanagisawa, and K. Nishinari, Phys. Rev. E **86**, 026118 (2012).

[13] A. Jelić, C. Appert-Rolland, S. Lemercier, and J. Pettré, Phys. Rev. E **86**, 046111 (2012).

[14] D. Yanagisawa, A. Tomoeda, and K. Nishinari, Phys. Rev. E **85**, 016111 (2012).

[15] K. Bhattacharya and T. Vicsek, New J. Phys. **12**, 093019 (2010).

[16] P. Romanczuk, I. D. Couzin, and L. Schimansky-Geier, Phys. Rev. Lett. **102**, 010602 (2009).

[17] K. Nishinari, D. Chowdhury, and A. Schadschneider, Phys. Rev. E **67**, 036120 (2003).

[18] M. Bando, K. Hasebe, A. Nakayama, A. Shibata, and Y. Sugiyama, Phys. Rev. E **51**, 1035 (1995).

[19] Y. Kuramoto, *Chemical Oscillations, Waves and Turbulence* (Springer-Verlag, Berlin, 1984).

[20] A. H. Cohen, P. J. Holmes, and R. H. Rand, J. Math. Biol. **13**, 345 (1982).

[21] J. A. Acerbrón, L. L. Bonilla, C. J. Pérez-Vicente, F. Ritort, and R. Spigler, Rev. Mod. Phys. **77**, 137 (2005).

[22] We can obtain this condition by substituting the expansions $\epsilon_n = \sum E_k \exp(\mathbf{i}kn + zt)$ and $\delta_n = \sum D_k \exp(\mathbf{i}kn + zt)$, and putting $z < 0$. See also Ref. [18].

[23] S. H. Strogatz, D. M. Abrams, A. McRobie, B. Eckhardt, and E. Ott, Nature (London) **438**, 43 (2005).

[24] B. Eckhardt, E. Ott, S. H. Strogatz, D. M. Abrams, and A. McRobie, Phys. Rev. E **75**, 021110 (2007).

[25] A. Nakayama, K. Hasebe, and Y. Sugiyama, Phys. Rev. E **71**, 036121 (2005).